

# Plasmonic Excitations in Tight-Binding Nanostructures

Rodrigo A. Muniz\* and Stephan Haas

*Department of Physics and Astronomy,*

*University of Southern California, Los Angeles, CA 90089-0484*

A.F.J. Levi

*Department of Electrical Engineering,*

*University of Southern California, Los Angeles, CA 90089-0082*

Ilya Grigorenko

*Theoretical Division T-11, Center for Nonlinear Studies,*

*Center for Integrated Nanotechnologies,*

*Los Alamos National Laboratory, Los Alamos, New Mexico 87545, USA*

(Dated: February 3, 2022)

## Abstract

We explore the collective electromagnetic response in atomic clusters of various sizes and geometries. Our aim is to understand, and hence to control, their dielectric response, based on a fully quantum-mechanical description which captures accurately their relevant collective modes. The electronic energy levels and wave functions, calculated within the tight-binding model, are used to determine the non-local dielectric response function. It is found that the system shape, the electron filling and the driving frequency of the external electric field strongly control the resonance properties of the collective excitations in the frequency and spatial domains. Furthermore, it is shown that one can design spatially localized collective excitations by properly tailoring the nanostructure geometry.

## I. INTRODUCTION

Recent advances in nanoscience have created a vast number of experimentally accessible ways to configure atomic and molecular clusters into different geometries with strongly varying physical properties. Specifically, exquisite control of the shape and size of atomic and molecular clusters has made it now possible to investigate the collective electromagnetic response of ultra-small metal and semiconductor particles.<sup>1,2</sup> The aim of this study is to model and examine plasmonic excitations in such structures, and thus to gain an understanding of the quantum-to-classical crossover of collective modes with increasing cluster size. There is obvious technological relevance to tunable collective modes in nanostructures. For example, surface plasmon resonances in metallic nanospheres and films have been found to be highly sensitive to nearby microscopic objects, and hence are currently investigated for potential sensing applications.<sup>3</sup> In this context, it is desirable to design customized nanostructures with specifically tailored resonance properties,<sup>4</sup> and this study is intended to be a first step into this direction.

It is natural to expect that in many cases the electromagnetic response of nanoclusters is considerably different from the bulk. In particular for very small clusters, the quantum properties of electrons confined in the structure need to be taken into account. Moreover, unlike in the bulk, the coupling between single-particle excitations and collective modes can be very strongly affected by its system parameters. This exponential sensitivity opens up excellent opportunities to optimize the dielectric response via tuning the cluster geometry and its electron filling. For example, by proper arrangement of atoms on a surface one can design nanostructures with controllable resonances in the near-infrared or visible frequency range.<sup>2</sup> A possible application of such nanostructures is the creation of metamaterials with negative refractive index at a given frequency. Furthermore, since geometry optimization of bulk resonators has demonstrated minimization of losses in metamaterials<sup>5</sup>, it is also interesting to investigate the effect of the nanostructure shape on the loss function at a given resonance frequency.

To approach this problem, in this study we investigate the formation of resonances in generic systems of finite conducting clusters, and examine how their frequency and spatial dielectric response depends on the system size and geometry. In particular, the non-locality of the dielectric response function in these structures is important, and will therefore be

properly accounted for. A similar analysis for the case of small *metallic* nanostructures was performed recently, using an effective mass approximation.<sup>6</sup> Here we focus on the opposite limit, namely we assume that electrons in the cluster can be effectively described using a tight-binding model.<sup>7</sup> Because of the more localized nature of the electronic wave functions in this model the overall magnitude of the collective modes are expected to be strongly suppressed as compared to metallic clusters.

This paper is organized in the following way. In the next section we introduce the model and method. For a more extended discussion, the reader is referred to Ref.<sup>6</sup>. Results for the induced energy as a function of the driving frequency of an externally applied electric field and the corresponding spatial modulations of the charge density distribution function are discussed in the following section. Finally, a discussion of possible extensions and applications is given in the conclusion section.

## II. MODEL

The interaction of electromagnetic radiation with nanoscale conducting clusters is conventionally described by semi-classical Mie theory.<sup>8</sup> This is a local, continuum-field model which uses empirical values of the linear optical response of the corresponding bulk material, and has been applied in nanoparticles to describe plasmon resonances.<sup>9</sup> However, such a semi-empirical continuum description breaks down beyond a certain degree of roughness introduced by atomic length scales, and thus cannot be used to describe ultra-small systems. In addition, near-field applications, such as surface-enhanced Raman scattering,<sup>10</sup> are most naturally described using a real-space theory which includes the non-local electronic response of inhomogeneous structures. Therefore, we will use a recently developed self-consistent and fully quantum-mechanical model which fully accounts for the non-locality of the dielectric response function.<sup>6</sup>

Specifically, to identify the plasmonic modes in small clusters we calculate the total induced energy due to an applied external electric field with driving frequency  $\omega$ , and scan for the resonance peaks. The induced energy is determined within the non-local linear response approximation.

To keep the computational complexity of this procedure at a minimum, we use a one-band tight-binding model to obtain the electronic energy levels  $E_i$  and wave functions  $\psi_i(\mathbf{r})$

as a linear combination of s-orbitals

$$\psi_i(\mathbf{r}) = \sum_{i,j} \alpha_{ij} \varphi(\mathbf{r} - \mathbf{R}_j), \quad (1)$$

where  $\varphi(\mathbf{r} - \mathbf{R}_j)$  is the wave function of a s-orbital around an atom localized at position  $\mathbf{R}_j$  and  $\alpha_{ij}$  are the coefficients of the eigenvector (with energy  $E_i$ ) of the Hamiltonian, which has the matrix elements

$$\langle \varphi(\mathbf{r} - \mathbf{R}_i) | H | \varphi(\mathbf{r} - \mathbf{R}_j) \rangle = \begin{cases} \mu & i = j \\ -t & i, j \text{ n.n.} \\ 0 & \text{otherwise} \end{cases} \quad (2)$$

Here  $t$  is the tight-binding hopping parameter. The Hamiltonian matrix is diagonalized using the Householder method to first obtain a tridiagonal matrix and then a QL algorithm for the final eigenvectors and eigenvalues.<sup>11</sup>

Once the electronic wave functions have been obtained, it is possible to calculate the dielectric susceptibility  $\chi(\mathbf{r}, \mathbf{r}', \omega)$  via

$$\chi(\mathbf{r}, \mathbf{r}', \omega) = \sum_{i,j} \frac{f(E_i) - f(E_j)}{E_i - E_j - \omega - i\gamma} \psi_i^*(\mathbf{r}) \psi_i(\mathbf{r}') \psi_j^*(\mathbf{r}') \psi_j(\mathbf{r}). \quad (3)$$

The induced charge density distribution function is then obtained by

$$\rho_{ind}(\mathbf{r}, \omega) = \int \chi(\mathbf{r}, \mathbf{r}', \omega) (\phi_{ind}(\mathbf{r}', \omega) + \phi_{ext}(\mathbf{r}', \omega)) d\mathbf{r}', \quad (4)$$

where in turn the induced potential is given by

$$\phi_{ind}(\mathbf{r}, \omega) = \int \frac{\rho_{ind}(\mathbf{r}', \omega)}{|\mathbf{r} - \mathbf{r}'|} d\mathbf{r}'. \quad (5)$$

We avoid the large memory requirement to store  $\chi(\mathbf{r}, \mathbf{r}', \omega)$  by calculating the induced charge density distribution iteratively via

$$\rho_{ind}(\mathbf{r}, \omega) = \sum_{i,j} \frac{f(E_i) - f(E_j)}{E_i - E_j - \omega - i\gamma} \psi_i^*(\mathbf{r}) \psi_j(\mathbf{r}) \int \psi_i(\mathbf{r}') \phi_{tot}(\mathbf{r}', \omega) \psi_j^*(\mathbf{r}') d\mathbf{r}', \quad (6)$$

with  $\phi_{tot}(\mathbf{r}', \omega) = \phi_{ind}(\mathbf{r}', \omega) + \phi_{ext}(\mathbf{r}', \omega)$ . The integrals are evaluated using a 4<sup>th</sup> order formula obtained from a combination of Simpson's Rule and Simpson's 3/8 Rule. Eqs. 5 and 6 are solved self-consistently by iterating  $\phi_{ind}(\mathbf{r}, \omega)$  and  $\rho_{ind}(\mathbf{r}, \omega)$ . This procedure typically converges in 3-8 steps when starting with  $\phi_{ind}(\mathbf{r}, \omega) = 0$ , depending on the proximity to

a resonance and on the value of the damping constant  $\gamma$ , which throughout this paper is chosen as  $\gamma = 0.08t$ . A much better performance can be achieved when the initial  $\phi_{ind}(\mathbf{r}, \omega)$  is taken as the solution of a previously solved nearby frequency. Upon its convergence, the frequency and spatial dependence of the induced electric field and the induced energy are obtained using

$$\mathbf{E}_{ind}(\mathbf{r}, \omega) = -\nabla\phi_{ind}(\mathbf{r}, \omega) \quad (7)$$

and

$$U_{ind}(\omega) = \int |\mathbf{E}_{ind}(\mathbf{r}, \omega)|^2 d\mathbf{r} \quad (8)$$

The observed resonances in the induced energy and charge density distribution at certain driving frequencies of the applied electric field correspond to collective modes of the cluster. In the following, the local induced charge density distribution is used for analyzing the characteristic spatial modulation of a given plasmonic resonance.

### III. RESULTS

Let us first focus on the dielectric response function in linear chains of atoms, with the intent to identify the basic features of their collective excitations. The frequency dependence of the induced energy in such systems, exposed to a driving electric field along the chain direction, is shown in Fig.1(a). It exhibits a series of resonances, which increase in number for chains with increasing length. As observed in the spatial charge density distribution, e.g. shown for the 5-atom chain in Fig.1(b), the lowest peak corresponds to a dipole resonance. When increasing the system size, the dipole peak moves to lower frequencies, which is the expected finite-size scaling behavior. The resonances at higher frequency correspond to higher harmonic charge density distributions. For example, in Fig.1(c), we show the charge density distribution corresponding to the highest frequency resonance of the 6-atom chain. In contrast to the dipole resonance, these modes show a rapidly oscillating charge density distribution, and thus have the potential to provide spatial localization of collective excitations in more sophisticated structures. While an extension to much larger chains is numerically prohibitive within the current method, the finite-size scaling of the observed dielectric response of these clusters is consistent with the 1D bulk expectation of a dominant low-energy plasmon mode, coexisting with a particle-hole continuum of much weaker spectral intensity.

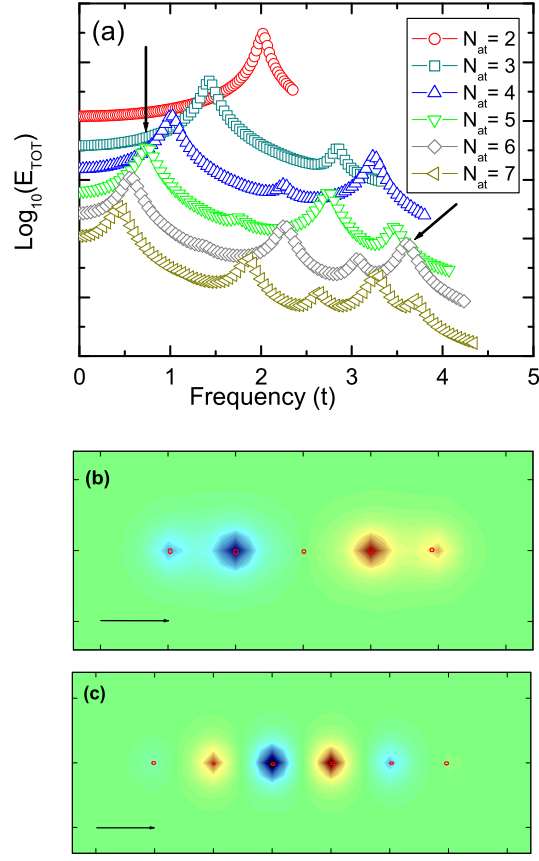


FIG. 1: Longitudinal modes in atomic chains. (a) Decimal logarithm of the total induced energy (artificially offset) as a function of the frequency of an external electric field which is applied along the direction of the chain. The resonance peaks correspond to different modes. (b) Induced charge density distribution for the lowest energy mode at  $\omega = 0.73t$  in the 5-atom chain. (c) Induced charge density distribution for the highest-energy mode at  $\omega = 3.56t$  in the 6-atom chain.

In order to study the transverse collective modes we apply an external electric field perpendicular to ladder structures made of coupled linear chains of atoms.<sup>12</sup> Fig.2(a) shows that for every chain size there are two resonance peaks for the total induced energy, the higher energy is an end mode, as shown in Figs.2(b) and (c) for the 3 and 5-atom double chains respectively, whereas the lower energy peak corresponds to a central mode, as displayed in Fig.2(d) for the 6-atom double chain. It is also confirmed that as the length of the chain is increased, the central mode gets stronger relatively to the end mode, which is the expected behavior for bulk vs. surface excitations. These results are in agreement with the findings

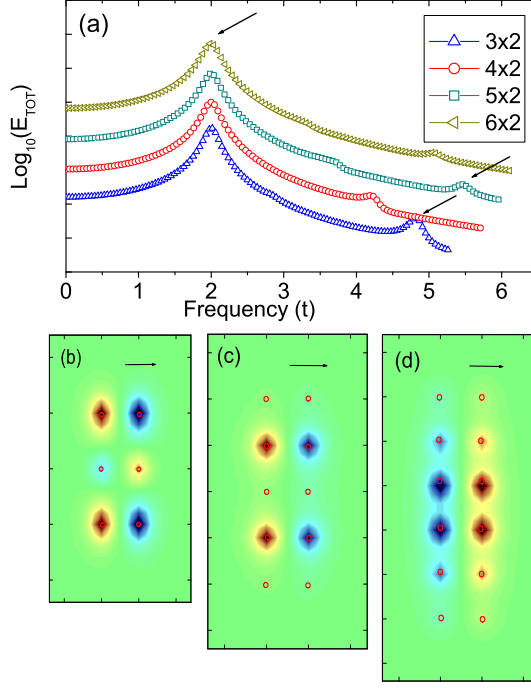


FIG. 2: Transverse Modes in coupled chain structures. (a) Logarithm of the total induced energy (artificially offset) as a function of the frequency of an external electric field applied transversely to the chain. The low energy mode is central, the analog of a bulk plasmon, and the high energy mode is located at the surface, the analog of a surface plasmon. (b) Induced charge density distribution for the mode at  $\omega = 4.91t$  in the 3-atom double chain. (c) Induced charge density distribution for  $\omega = 5.41t$  in the 5-atom double chain. (d) Induced charge density distribution for  $\omega = 1.93t$  in the 6-atom double chain.

of Ref.<sup>13</sup>.

Let us next examine what happens when the direction of the external electric field is varied. Fig.3 shows the dielectric response of a  $4 \times 6$ -atom rectangular structure for different angles incidence directions of the applied field. When the field is parallel to one of the edges ( $\theta = 0^\circ$  or  $\theta = 90^\circ$ ), the response is essentially that of a single chain with the same length, shown in Fig.1(a). Also the induced spatial charge density modulations are analogous to those of the correspondent linear chain, which can be seen in Figs. 3(b) and (c). At intermediate angles the response is a superposition of the two above cases, changing gradually from one extremum to the other as the angle is changed. Notice for instance that as the

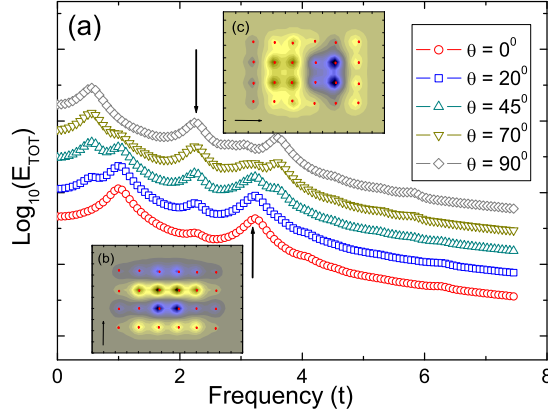


FIG. 3: Dependence on the direction of the applied electric field. (a) Logarithm of the total induced energy (artificially offset) as a function of frequency of external electric fields applied to a  $4 \times 6$ -rectangle at different incident angles.  $\theta = 0^\circ$  when the field is parallel to the 4-atoms edge, and  $\theta = 90^\circ$  when it is parallel to the 6-atoms edge. (b) Induced charge distribution for  $\theta = 0^\circ$  and  $\omega = 3.15t$ . (c) Induced charge density distribution for  $\theta = 90^\circ$  and  $\omega = 2.15t$ .

angle increases, the peak at the same frequency of the 4-atoms dipole resonance diminishes, while simultaneously another resonance is formed at the frequency of the dipole mode of a 6-atoms chain when the angle is tuned from  $\theta = 0^\circ$  to  $\theta = 90^\circ$ . For  $\theta = 0^\circ$  there is only the peak at the frequency of the 4-atom chain dipole resonance, whereas for  $\theta = 90^\circ$  only the dipole peak corresponding to the 6-atoms dipole frequency is present. The superposition of the responses from each direction is a consequence of the linear response approximation employed, since the response is a linear combination of those obtained from each direction component of the external field.

Next, let us analyze the dependence of the resonance modes on the number of electrons in the cluster. Fig.4(a) shows significant changes in the response of a 9-atom chain with the external field applied along its direction. In particular, it is observed that the response is stronger when there are more electrons in the sample, a quite obvious fact since there are more particles contributing to the collective response. Moreover the resonance frequencies of lower modes increase with the number of electrons, which can be understood as a consequence of the one-dimensional tight-binding density of states being smallest at the center of the band. Hence the energy levels around the Fermi energy are more sparse in the finite



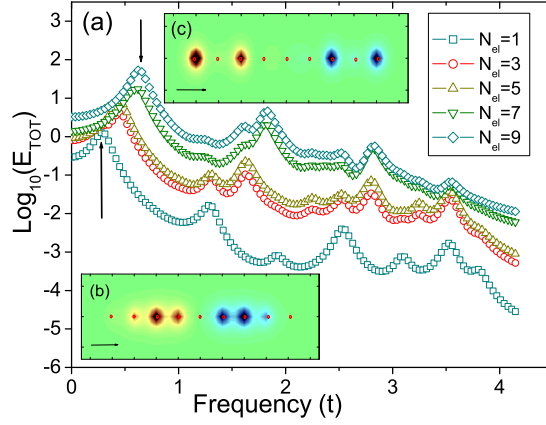


FIG. 4: Variation of the number of electrons. (a) Logarithm of the total induced energy as a function of the external electric field frequency. The number of electrons  $N_{el}$  in a 9-atom chain is varied. (b) Induced charge density distribution for  $N_{el} = 1$  at  $\omega = 0.36t$ . (c) Induced charge density distribution for  $N_{el} = 9$  at  $\omega = 0.53t$ .

system, and therefore the excitations require larger frequencies at half-filling. The same does not hold for higher frequency modes since these correspond to transitions between the lowest and highest levels for any number of electrons in the sample. Therefore these modes have the same frequency, independent of the electronic filling. Higher filling also allows the induced charge density to concentrate closer to the boundaries of the structure, as a comparison between Figs.4(b) and (c) demonstrates. Fig.4(b) shows that a 9-atoms chain with  $N_{el} = 1$  electron has its induced charge density localized around the center of the chain. In contrast, Fig.4(c) displays the induced charge density localized at the boundaries of the same structure with  $N_{el} = 9$ . This concentration closer to the surface happens because higher energy states have a stronger charge density modulation than the lower energy ones. Therefore the induced charge density is more localized for higher fillings, because at low fillings the excitations responsible for the induced charge density are between the more homogeneous lower energy levels. This can be interpreted as a finite-size rendition of the fact that by increasing the electronic filling one obtains the classical response with all the induced charge density on the surface of the object.

Access to high energy states is very important for achieving spatial localization of the induced charge density, as the next example shows. In order to find a structure with spatially

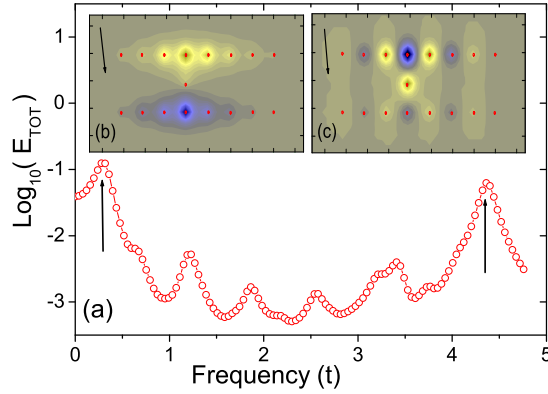


FIG. 5: Connect between two chains,  $N_{el} = 1$ . (a) Logarithm of the total induced energy as a function of the frequency of an external electric field applied to two 8-atom chains with an extra atom connecting them at the center. (b) Induced charge density distribution for  $\omega = 2.28t$ . (c) Induced charge density distribution for  $\omega = 4.36t$ .

localized plasmons we consider two parallel 8-atoms chains connected to each other by an extra atom at the center. When an external electric field is applied transversely to the chains, the electrons are stimulated to hop between them, but this is only realizable through the connect, therefore the plasmonic excitation is sharply localized around it. Fig.5(a) shows the response of two 8-atoms chains, Fig.5(b) and (c) show respectively the induced charge density for the dipole and the highest modes. It is seen that the lowest frequency mode has a much longer spread along the chains, whereas the high frequency plasmon is sharper, since it corresponds to excitations to the highest energy state that has a large charge ondulation as it was pointed out before.

Let us finish by analyzing the dependence of the various dielectric response modes on the distance between atoms in the chain. The dipole moment of the chain is proportional to its length, and consequently also proportional to the distance between neighboring atoms. Hence one can expect that the strength of the dielectric response is also proportional to the atomic spacing. However, higher frequency modes require a larger mobility of electrons since they need to move quickly along the chain in order to produce the charge oscillations of the mode. In other words, the charge-density waves can only have frequencies at most equal to the wavering of the charge carriers. Hence the high frequency modes are suppressed for systems where electrons lack the mobility necessary for the execution of their oscillation.

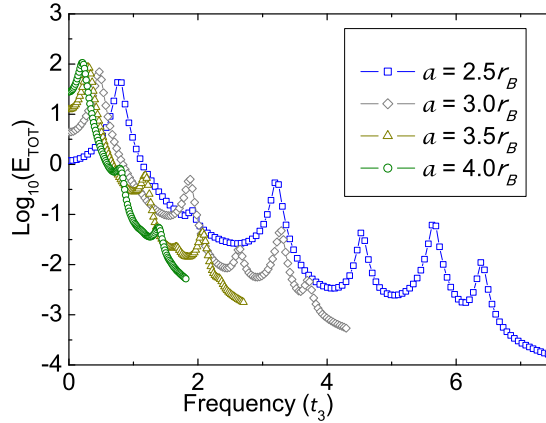


FIG. 6: Variation of the distance between neighbor atoms  $a$ . Logarithm of the total induced energy as a function of the frequency of an external electric field applied to 7-atom chains with different spacing between atoms  $a$  in units of the Bohr radius  $r_B$ . The frequency unit is  $t_3$  the tight-binding hopping parameter for  $a = 3r_B$ .

In the tight-binding model, the electronic mobility stems from the tunneling of electrons from one atom to another. The tunneling rate depends on the overlap of the atomic orbitals located in different sites, and moreover this overlap decays exponentially with the spacing between atoms. Therefore the high frequency modes are weaker for long spaced chains, while the slow modes get stronger. This fact is demonstrated in Fig.6 where the response of 7-atom chains with different atomic spacings are shown. The tight-binding hopping parameter  $t$  changes with the atomic spacing  $a$ , and here we considered a generic<sup>14</sup> power-law dependence  $t \sim a^{-3}$ . The figure clearly shows that the strength of the slowest mode is reduced for shorter spacings. The opposite is true for the two fastest modes, while the intermediate modes have nearly no change.

#### IV. CONCLUSION

In conclusion, we have analyzed the evolution of plasmonic resonances in small clusters as a function of the system shape, applied external fields, electron filling and atomic separation. Using a fully quantum-mechanical, non-local response theory, we observe that longitudinal and transverse modes are very sensitive to these system parameters. This is reflected in

their frequency, oscillator strength and the spatial modulation of the induced charge density. Specifically, we identify bulk and surface plasmonic excitations which can be controlled in amplitude and frequency by the cluster size. Furthermore, we observe a non-trivial filling dependence, which critically depends on the electronic level spacing in a given structure. We also find that changes in atomic spacings strongly affect the electron mobility in these structures, with a very different impact on low-energy vs. high-energy modes. And we see that changing the position of a single atom in a nanostructure can completely alter its collective dielectric response. This strong sensitivity to small changes is the key to controlling the modes of ultra-small structures, and it can thus become the gateway to a new generation of quantum devices which effectively utilize quantum physics for new functionalities.

### Acknowledgments

We would like to thank Gene Bickers, Richard Thompson, Vitaly Kresin, Aiichiro Nakano and Yung-Ching Liang for useful conversations, and we acknowledge financial support by the Department of Energy, grant number DE-FG02-06ER46319. The numerical computations were carried out on the University of Southern California high-performance computer cluster.

---

\* Electronic address: rmuniz@usc.edu

<sup>1</sup> V.V. Kresin, Phys. Rep. **220**, 1 (1992); K.D. Bonin and V.V. Kresin, “Electric-Dipole Polarizabilities of Atoms, Molecules and Clusters” (World Scientific, Singapore, 1997).

<sup>2</sup> G.V. Nazin, X.H. Oiu, and W. Ho, Science **302**, 77 (2003); G.V. Nazin, X.H. Oiu, and W. Ho, Phys. Rev. Lett. **90**, 216110 (2003); N. Nilius, T.M. Wallis, M. Persson, and W. Ho, Phys. Rev. Lett. **90**, 196103 (2003); N. Nilius, T.M. Wallis, and W. Ho, Science **297**, 1853 (2002).

<sup>3</sup> J. Homola, S.S. Yee, and G. Gauglitz, Sensors & Actuators: B **54**, 3 (1999).

<sup>4</sup> C.R. Moon, L.S. Mattos, B.K. Foster, G. Zeltzer, W. Ko, and H.C. Monoharan, Science **319**, 782 (2008).

<sup>5</sup> A. K. Sarychev and V. M. Shalaev, “Electrodynamics of Metamaterials” (World Scientific, Singapore, 2007).

<sup>6</sup> I. Grigorenko, S. Haas and A.F.J. Levi, Phys. Rev. Lett. **97**, 036806 (2006); A. Cassidy, I.

- Grigorenko, and S. Haas, Phys. Rev. B **77**, 245404 (2008); I. Grigorenko, S. Haas, A.V. Balatsky, and A.F.J. Levi, New J. Phys. **10**, 043017 (2008).
- <sup>7</sup> J.C. Slater and G.F. Koster, Phys. Rev. **94**, 1498 (1954); C.M. Goringe, D.R. Bowler and E. Hernandez, Rep. Prog. Phys. **60**, 1447 (1997); N. W. Ashcroft and N. D. Mermin, “Solid State Physics” (Thomson Learning, 1976).
- <sup>8</sup> G. Mie, Annalen der Physik, 25, 377 (1908).
- <sup>9</sup> D. M. Wood and W. R. Ashcroft, Phys. Rev. B 25, 6255 (1982); M. J. Rice, W. R. Schneider, and S. Strassler, Phys. Rev. B 8, 474 (1973); S. Das Sarma, Phys. Rev. B 43, 11768 (1991); D. R. Fredkin and L. D. Mayergoyz, Phys. Rev. Lett. 91, 253902 (2003).
- <sup>10</sup> S. Nie and S. R. Emory, Science 275, 1102 (1997).
- <sup>11</sup> W. H. Press, B. P. Flannery, S. A. Teukolsky, W. T. Vetterling, “Numerical Recipes” (Cambridge University Press, 1988).
- <sup>12</sup> Within the current approach, at least two coupled chains are necessary to visualize charge redistributions along the transverse direction, since charge fluctuations within the orbitals are not accounted for.
- <sup>13</sup> J. Yan, Z. Yuan and S. Gao, Phys. Rev. Lett. **98**, 216602 (2007).
- <sup>14</sup> W.A. Harrison, “Electronic Structure and the Properties of Solids” (W. H. Freeman, San Francisco, 1980).